Optimization of Maintenance Scheduling for Offshore Wind Turbines Considering the Wake Effect of Arbitrary Wind Direction

Xiaolin Ge [1], Quan Chen [1], Yang Fu [1*], C. Y. Chung [2], and Yang Mi [1]

[1] Electric Power College, Shanghai University of Electric Power, Shanghai, China
[2] The Department of Electrical and Computer Engineering, University of Saskatchewan, Saskatoon, SK S7N 5A9, Canada
[*]Corresponding author: mfudong@126.com

Abstract: **An optimization model for offshore wind farm maintenance scheduling is presented, considering minimum maintenance costs and maximum power generation. For power generation, the wind speed at each tower site plays an important role that is impacted not only by the dynamically changing wake overlap area and the consequence of variation of wind direction but also by the relative position of the wake affected by the maintenance status. This paper combines the wake model with the maintenance status to accurately express the input wind speed of the wind turbine (WT) in each period. Because the optimization model includes complex dynamical coupling relationships and a number of nonlinear constraints, mixed integer second-order cone programming (MISOCP) are employed to address these issues. The MISOCP model is relaxed as a mixed integer linear programming (MILP) model to improve computational efficiency and the ε-constraint method is utilized to handle the multi-objective function. The proposed model and method are tested in a short-term maintenance case of an offshore wind farm. The numerical results demonstrate that the proposed approach can achieve sound economic benefits and provide comprehensive decision support.**

Keywords： **offshore wind farm; maintenance; wake effect; mixed integer linear programming; multi-objective**

Nomenclature

Indexes and sets

i, j	Index of offshore WTs.
t	Index of time periods [h].
ω	Index of scenarios.

Parameters

m	Number of WTs in the offshore wind farm
n	Number of periods in time horizon
Ω	Number of scenarios after reduction
π_ω	Probability of scenario ω
$k_{j,i}$	Wake reduction coefficient of WT i to WT j
α	Wind direction [°]
$v0_{j,t}$	Input wind speed of WT j in period t assuming it is not affected by any wake [m/s]
$v0_{j,t,\omega}$	Input wind speed of WT j in period t under scenario ω assuming it is not affected by any wake [m/s]
$P^{\mathrm{b}}_{i,t,\omega}$	Predicted power output of WT i in period t under scenario ω [kW]
$A^{\mathrm{o}}_{j,i}$	Wake obstruction area of WT i to WT j [m^2]
$A^{\mathrm{o}}_{j,i,t}$	Wake obstruction area of WT i to WT j in period t [m^2]
A_j	Sweeping area generated by WT j [m^2]
$\eta_{j,i}$, $\eta_{j,i,t}$	Wake obstruction area ratio of $A^{\mathrm{o}}_{j,i}/A_j$ and $A^{\mathrm{o}}_{j,i,t}/A_j$
$\eta_{j,i,t,\omega}$	Wake obstruction area ratio of $A^{\mathrm{o}}_{j,i,t}/A_j$ under scenario ω
O_i	Center of WT i
O^{w}_i	Center of the wake that developed from upstream WT i
e_1	Angle between line O_i - O_j and y-axis [°]
$R_{j,i}$	Radius of the wake generated by WT i to WT j [m]
R_j	Impeller radius of WT j [m]
$L_{j,i}$	Distance between upstream WT i and downstream WT j [m]
$d_{j,i}$	Distance from O_j to O^{w}_i [m]
u_i	Maintenance duration required by WT i [h]
$c^{\mathrm{e}}_{i,t}$, $c^{\mathrm{g}}_{i,t}$	Material equipment and environmental monitoring cost for WT i in period t [$]
$c^{\mathrm{r}}_{i,t,\omega}$, $c^{\mathrm{y}}_{i,t,\omega}$	Transportation and manpower cost for WT i in period t under scenario ω [$]

c_t^{f}	Infrastructure cost in period t [$]
c^{v} , c^{h}	Unit vessel and helicopter fixed cost [$]
σ_i , θ_i	Vessel and helicopter demand for maintaining WT i
$c_{t,\omega}^{\mathrm{s}}$, $c_{t,\omega}^{\mathrm{z}}$	Unit vessel and helicopter transport cost in period t under scenario ω [$]
$c_{t,\omega}^{\mathrm{d}}$, $c_{t,\omega}^{\mathrm{q}}$, $c_{t,\omega}^{\mathrm{l}}$	Vessel, helicopter and onshore per capita manpower cost in period t under scenario ω [$]
δ_i^{v} , δ_i^{h} , δ_i^{l}	Vessel, helicopter and onshore manpower demand for WT i
w	Unit price of wind power [$/kW·h]
Δ_t	Duration of period t [h]
τ_i	Maintenance deadline of WT i
U_ω	Time period set not allowed for maintenance under scenario ω due to the weather
δ_t^{a} , θ_t^{a} , σ_t^{a}	Number of available manpower, helicopters and vessels in period t
D_i	Distance from shore to WT i [km]
q^{v}, q^{h}	Vessel and helicopter gas emissions [kg/kg·km]
ϑ	Average weight of an employee [kg]
z_i^{v} , z_i^{h}	Equipment on vessels and helicopters for WT i [kg]
GHG	Greenhouse gas emission standard regulated by the industry [kg]
σ_t^{p}	Permitted moving vessels in period t for protecting the marine environment
θ_t^{p}	Permitted moving helicopters in period t for protecting the lives of birds
Y	Time period set of daily night
ξ	Total time of vessels allowed to travel to the sea on daily night [h]
P_i^{r}	Rated power of WT i [kW]
v_i^{in} , v_i^{r} , v_i^{out}	Cut-in, rated and cut-out wind speed of WT i [m/s]
M	Sufficiently large positive number

Variables

f_1, f_2	Maintenance costs [$] and power generation [kWh] of the offshore wind farm
ε_γ	The constraint value of f_1 and f_2
$v_{i,t}$	Input wind speed of WT i in period t [m/s]

$v_{i,t,\omega}$	Input wind speed of WT i in period t under scenario ω [m/s]
$v_{j,i,t}$	Wake velocity of WT i wake effect on WT j in period t [m/s]
$v_{j,i,t,\omega}$	Wake velocity of WT i wake effect on WT j in period t under scenario ω [m/s]
$C_{i,t}^{\mathrm{T}}$	Thrust coefficient of WT i in period t
$C_{i,t,\omega}^{\mathrm{T}}$	Thrust coefficient of WT i in period t under scenario ω
$P_{i,t,\omega}$	Power output of WT i in period t under scenario ω [kW]
$W_{i,t,\omega}^{\mathrm{u}}$	Power loss due to shutdown of WT i in period t under scenario ω [kWh]
$c_{i,t,\omega}^{\mathrm{u}}$	Shutdown loss cost for WT i in period t under scenario ω [$]
$b_{i,t}$	0–1 decision variable denoting the starting state of WT i in period t
$I_{i,t}$	0–1 decision variable denoting the maintenance state of WT i in period t
$\varphi_{j,i,t,\omega}^{k}, \beta_{j,i,t,\omega}^{k}, v1_{j,i,t,\omega}, v2_{j,i,t,\omega}, v3_{j,t,\omega}$	Auxiliary variables
ζ	Slack variable

1. Introduction

Compared to onshore wind, offshore wind power has significant advantages including high average wind speed and utilization hours of power generation. However, harsh marine geography and poor accessibility introduce serious challenges to the maintenance of offshore wind turbines (WTs) [1]. Thus, the maintenance cost of offshore WTs is high and accounts for about 40% of the total lifetime cost of WTs [2]. Effective scheduling of wind generator maintenance can result in significant potential energy savings and economic benefits for offshore wind farms. Many researchers have focused on this issue in the past decade.

The approaches of maintenance for WTs can be mainly classified into two types: maintenance scheduling [3-6] and fault detection and diagnosis [7-11]. Studies on the short-term maintenance scheduling of offshore wind generators mainly aim to optimize the maintenance starting times in the marine operating environment. A maintenance management system is described and a maintenance path with minimum cost for onshore and offshore wind farms is presented in [3]. Maintenance scheduling of

an offshore wind farm is improved by condition monitoring systems in [4]. Technicians with different skills are coordinated to increase the efficiency of short-term maintenance scheduling in [5, 6]. Notably, in the abovementioned research the objective of maintenance scheduling is simply to minimize maintenance costs. Power generation benefits are not taken into account in the studied time horizon, which will lead to a decline in the utilization of offshore wind resources. Maintenance scheduling of onshore wind power considering both power generation and maintenance costs was proposed in [12, 13]. However, due to differences between offshore and onshore WTs in terms of operating environment, maintenance modes, and accessibility, existing optimization models are not applicable to offshore wind power.

Because the wind direction continuously changes, the position of downstream WTs varies in a corresponding fashion and the wake effect among the WTs will also change. Thus, the wake effect reflects the coupling between the upper and lower WTs and the varied wind direction means the coupling changes. Due to the complex relationship, the wake effect is omitted when analyzing the output power of wind farms to simplify the calculation [14]. Some studies calculate the wind farm output with the wake in a single wind direction [15, 16]. To consider the influence of wind direction, wake coefficient is used to evaluate the impact of the wake effect on the output power of the wind farm in [17], which indicates the dependence of the wake coefficient upon wind direction. However, in scheduling problems, the characteristic of wake effect changing with wind directions [18-20] is often ignored. Therefore, a general wake model for any wind direction still needs to be considered in the maintenance scheduling.

Furthermore, when the WT is in maintenance, it does not absorb wind energy and the wake distribution of the wind farm is affected. Considering the arbitrariness and randomness of the wind direction, the coupling among WTs changes in both spatial and temporal dimensions. This makes short-term maintenance scheduling very complicated, and generally formulated as a dynamic coupling, multi-objective, multi-constraint nonlinear stochastic programming problem. Many intelligent algorithms have been utilized to solve this problem, such as ant colony system (ACO) [21], genetic algorithm (GA) [22], particle swarm optimization (PSO) [23], and non-dominated sorting genetic algorithm II (NSGA-

II) [24]. Additionally, dynamic programming (DP) [25], mixed integer linear programming (MILP) [26], mixed integer second-order cone programming (MISOCP) [27], mixed integer nonlinear programming (MINLP) [28], scenario analysis [29], the ε-constraint method [30], and other traditional methods have been successfully developed to deal with the complicated models. As pointed out in [31], intelligent algorithms are apt to converge to a local optimal solution when solving large scale multi-constraint problems. MILP solvers facilitate an easier formulation and a flexible approach for discrete decision making, and also have a higher commercial maturity. MILP has been widely applied to solve such problems [26, 31-34]. However, the wake effect is nonlinear and dynamically changing, and how to transform the wake effect into MILP models in short-term maintenance scheduling is still very challenging.

The comparison between the existing works and the proposed approach about offshore wind farm maintenance scheduling is reported in Table 1.

Table 1

Comparison of between the existing and proposed methods

No.	Ref.	Objective	Wind speed and direction	Factors considered	Modeling
1	[5]	Maintenance cost, power generation	Deterministic	Equipment, personnel, weather	Multivariate auto-regressive
2	[6]	Maintenance cost	Deterministic	Equipment, personnel, weather	Two-stage adaptive large neighborhood search
3	[24]	Maintenance cost, reliability	Deterministic	Equipment, personnel, weather, environmental protection	Multi-constrained non-linear programming
4	[35]	Net profit	Deterministic	Personnel, weather, WTs remaining life	Adaptive opportunistic maintenance and operations scheduling
5	[36]	Maintenance cost	Deterministic	Equipment, personnel, weather	MILP
6	[37]	Maintenance cost	Deterministic	Equipment, personnel, weather	Multi-constrained non-linear programming
7	[38]	Maintenance cost	Deterministic	Equipment, personnel, weather, unexpected failure of WTs	Simulation-based optimisation
8	[39]	Maintenance cost	Deterministic	Equipment, personnel, weather	Non-deterministic polynomial
9	[40]	Maintenance cost	Deterministic	Equipment, personnel, weather, maintenance accommodation	Maintenance support organization
10	Proposed approach	Maintenance cost, power generation	Uncertainty	Equipment, personnel, weather, environmental protection, wake effect in arbitrary wind direction	MILP

Similar to the most research works, this paper considers equipment, personnel, and weather constraints during maintenance scheduling. However, differing from the existing works, this paper considers a new important factor, the uncertainty of wind speed and direction, to make the obtained maintenance scheduling more feasible. Other advantages of current paper include that the influence of wind direction and maintenance status on the wake effect is considered in the maintenance scheduling model, and the proposed model is transformed into an easily-solved MILP model, which are not mentioned in existing works in Table 1. Simultaneously, for making full use of offshore wind resources and ensuring good economics, the bi-objective of power generation maximization of the offshore wind farm and maintenance costs minimization is presented, which is not included in [6, 35-40].

The main contributions of this paper are as follows:

1) Considering the dynamic influence of maintenance on wake distribution, a general wake model of arbitrary wind direction combined with maintenance state is proposed. In this model, the spatial and temporal coupling between downstream WTs and multi-upstream WTs is depicted. Thus, the changes of wake caused by wind direction and maintenance condition are considered, and the input wind speed of WTs is accurately calculated.

2) In the proposed maintenance scheduling optimization model, uncertainty of wind speed and direction are introduced to evaluate the maintenance cost and the power generation, to construct the objectives. The model considers output power, weather, and other maintenance-related constraints to address the prominent characteristic that the maintenance scheduling of offshore WTs is affected by wind condition, and achieves a more reasonable economic evaluation.

3) The quadratic terms in the model are transformed to second-order cones by the relaxation method. Based on this, the nonlinear part of the wake model as well as the relationship between the thrust coefficient and the input wind speed of the WT are handled by MISOCP. In addition, the above MISOCP model and the coupling functions of integer variables and continuous variables are converted into a MILP model by an algebraic modeling method to improve the computational efficiency.

The reminder of this paper is organized as follows. Section 2 states the establishment of the wake model. The optimization model of maintenance scheduling is formulated in Section 3 and its solution method is presented in Section 4. Section 5 provides numerical results from case studies. Conclusions are drawn in Section 6.

2. Wake effect

Subject to the area of the offshore wind farm, the spacing between WTs is relatively small, but the wake effect still significantly affects the input wind speed of the downstream WTs [41]. Assumed the arrangement of offshore WTs is as shown in Fig. 1, where the WTs in the wind farm are numbered from 1 to m and the coordinates (x_i, y_i) indicate the position of WT i relative to the original point. $i1_{max}$ represents the last WT in the first column.

To accurately obtain the input wind speed of the WT for any wind direction during the maintenance period, and depending on the law of conservation of kinetic energy of the airflow per unit time, the input wind speed of WT j in period t can be formulated as:

$$v_{j,t} = \sqrt{v0_{j,t}^2 + \sum_{i=1}^{m}\left[(1-I_{i,t})\eta_{j,i,t}(v_{j,i,t}^2 - v0_{j,t}^2)\right]} \tag{1}$$

As described in (1), the input wind speed of WT j is related to the maintenance state $I_{i,t}$, wake velocity $v_{j,i,t}$ of upstream WTs, and wake obstruction area ratio $\eta_{j,i,t}$. The wind speed that arrives at the blade of downstream WTs is affected by several upstream WTs. And, when the ambient wind direction changes between 0° and 360°, the wake obscuration area between upstream and downstream WTs varies. In addition, it can be found that, if WT i is maintained $I_{i,t}$=1, the wake effect from WT i to WT j is ignored, and otherwise, the wake effect from WT i to WT j should be considered. Therefore, the presented model represents the combination of the wake model and the maintenance status. Besides, $v_{j,i,t}$ can be obtained referring to [42], which can be expressed by (2).

$$v_{j,i,t} = v_{i,t}(1-k_{j,i}C_{i,t}^{\mathrm{T}}) \tag{2}$$

And wake obstruction area ratio $\eta_{j,i,t}$ is formulated by (3).

$$\eta_{j,i,t} = \frac{A^{o}_{j,i,t}}{A_j} \tag{3}$$

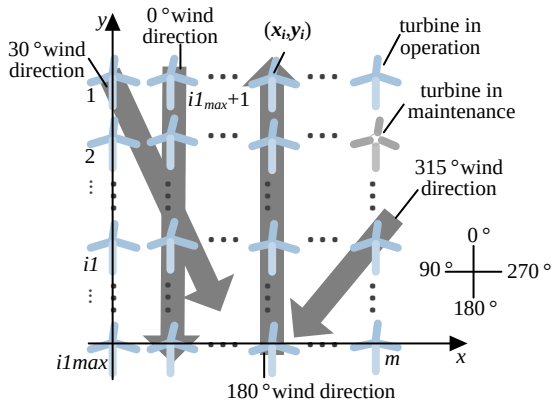

Fig. 1. The arrangement of offshore WTs

To calculate the wake obstruction area ratio $\eta_{j,i,t}$ in an arbitrary wind direction, the wake effect between WTs is illustrated in Fig. 2. Assuming that the wind direction is α in period t and WT j is overlapped with the right half of the wake plane, some distance parameters can then be expressed as:

$$L_{j,i} = \sqrt{(x_i - x_j)^2 + (y_i - y_j)^2} \tag{4}$$

$$d_{j,i} = L_{j,i} \left|\sin(e_1 - \alpha)\right| \tag{5}$$

$$R_{j,i} = R_i + k^{o} L_{j,i} \left|\cos(e_1 - \alpha)\right| \tag{6}$$

where (4) is the distance between upstream WT i and downstream WT j, (5) formulates the distance from O_j to O_i^{w}, and (6) represents the radius of the wake generated by WT i to WT j. k^{o} is the wake decay constant and the recommended value for an offshore environment is 0.04 [20].

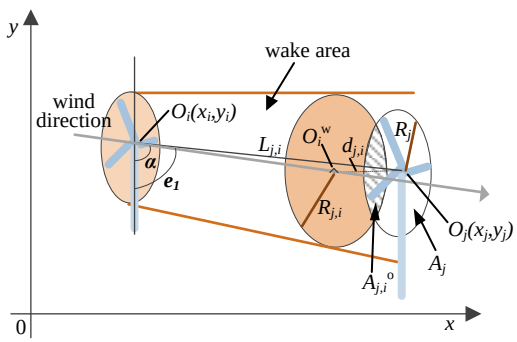

Fig. 2. Wake model with varying wind direction

When $0 \le d_{j,i} \le R_{j,i} - R_j$, it corresponds to the full wake effect and $\eta_{j,i}$ is equal to 1, while $d_{j,i} \ge R_{j,i} + R_j$ corresponds to the non-wake effect and $\eta_{j,i}$ is equal to 0. $R_{j,i} - R_j < d_{j,i} < R_{j,i} + R_j$

corresponds to the partial wake effect. In this case, $\eta_{j,i}$ can be formulated by (7) based on the method described in [23].

$$\eta_{j,i}=\left(R_{j,i}^{2}\cos^{-1}\frac{R_{j,i}^{2}+d_{j,i}^{2}-R_{j}^{2}}{2R_{j,i}d_{j,i}}+R_{j}^{2}\cos^{-1}\frac{R_{j}^{2}+d_{j,i}^{2}-R_{j,i}^{2}}{2R_{j}d_{j,i}}-d_{j,i}R_{j}\left|\sin(\arccos\frac{R_{j}^{2}+d_{j,i}^{2}-R_{j,i}^{2}}{2R_{j}d_{j,i}})\right|\right)\Big/\left(\pi R_{j}^{2}\right) \quad (7)$$

And similarly, when the left half of the wake plane overlaps with WT *j*, $\eta_{j,i}$ can also be obtained.

3. Model formulation

Wind speed and wind direction prediction have uncertainty. To improve the feasibility of maintenance scheduling, a stochastic programming model is proposed. The prediction value of wind speed and direction for each time period is assumed to obey the normal distribution [41, 43]. Based on this, the Latin hypercube sampling (LHS) method [44] is used to sample for generating scenarios, and then the scenario reduction method [45] is conducted to reduce the quantity of acquired samples to obtain prediction data for wind speed and direction of each scenario ω, and thus the uncertainty of wind speed and direction can be described by these scenarios.

3.1. Objective Functions

The maintenance cost of the offshore wind farm is high, and the maintenance scheduling should ensure good economics. Meanwhile, making full use of offshore wind resources to generate electricity to ensure wind farm revenue is also significant. Therefore, the objective of maintenance scheduling for the offshore wind farm is to minimize maintenance costs f_1 and maximize power generation f_2 over the studied time horizon.

1) Maintenance costs minimization

$$\min f_1=\min\sum_{i=1}^{m}\sum_{t=1}^{n}\left(\frac{c_{i,t}^{\mathrm{e}}+c_{i,t}^{\mathrm{g}}+c_{t}^{\mathrm{f}}}{u_i}+\sum_{\omega=1}^{\Omega}\pi_{\omega}(c_{i,t,\omega}^{\mathrm{r}}+c_{i,t,\omega}^{\mathrm{y}}+c_{i,t,\omega}^{\mathrm{u}})\right)I_{i,t}\,. \quad (8)$$

$c_{i,t,\omega}^{\mathrm{r}}$, $c_{i,t,\omega}^{\mathrm{y}}$, and $c_{i,t,\omega}^{\mathrm{u}}$ are expressed by

$$c_{i,t,\omega}^{\mathrm{r}}=\frac{c^{\mathrm{v}}\sigma_i+c^{\mathrm{h}}\theta_i}{u_i}+c_{t,\omega}^{\mathrm{s}}\sigma_i+c_{t,\omega}^{\mathrm{z}}\theta_i \quad (9)$$

$$c_{i,t,\omega}^{\mathrm{y}} = c_{t,\omega}^{\mathrm{d}}\delta_i^{\mathrm{v}} + c_{t,\omega}^{\mathrm{q}}\delta_i^{\mathrm{h}} + c_{t,\omega}^{\mathrm{l}}\delta_i^{\mathrm{l}} \tag{10}$$

$$c_{i,t,\omega}^{\mathrm{u}} = W_{i,t,\omega}^{\mathrm{u}} w \tag{11}$$

(8) indicates the expectation of maintenance costs for multi-scenarios.

2) Power generation maximization

$$\max\ f_2 = \max \sum_{\omega=1}^{\Omega}\sum_{i=1}^{m}\sum_{t=1}^{n} \pi_\omega P_{i,t,\omega}\Delta_t \tag{12}$$

As demonstrated in (12), the generation benefit of the wind farm in this paper is expressed as the expectation of power generation.

3.2. Constraints

The above objective functions are subject to the following constraints:

$$P_{i,t,\omega} \le (1 - I_{i,t})P_{i,t,\omega}^{\mathrm{b}} \tag{13}$$

$$\sum_{t=1}^{n} b_{i,t} = 1 \tag{14}$$

$$I_{i,t} \ge b_{i,t} \tag{15}$$

$$I_{i,t} - I_{i,t-1} \le b_{i,t} \tag{16}$$

$$I_{i,t} + I_{i,t-1} + b_{i,t} \le 2 \tag{17}$$

$$\sum_{t=1}^{n} I_{i,t} = u_i \tag{18}$$

$$I_{i,t} + I_{j,t} \le 1, \quad i \ne j \tag{19}$$

$$\sum_{t=1}^{\tau_i - u_i + 1} b_{i,t} = 1 \tag{20}$$

$$\sum_{t \in U_\omega} I_{i,t} = 0 \tag{21}$$

$$\sum_{i=1}^{m} (\delta_i^{\mathrm{v}} + \delta_i^{\mathrm{h}} + \delta_i^{\mathrm{l}}) I_{i,t} \le \delta_t^{\mathrm{a}} \tag{22}$$

$$\sum_{i=1}^{m} \sigma_i I_{i,t} \le \sigma_t^{\mathrm{a}} \tag{23}$$

$$\sum_{i=1}^{m} \theta_i I_{i,t} \le \theta_t^{\mathrm{a}} \tag{24}$$

$$\sum_{i=1}^{m} 2D_i b_{i,t}[q^{\mathrm{v}}(\vartheta\delta_i^{\mathrm{v}} + z_i^{\mathrm{v}}) + q^{\mathrm{h}}(\vartheta\delta_i^{\mathrm{h}} + z_i^{\mathrm{h}})] \le GHG \tag{25}$$

$$\sum_{i=1}^{m} \sigma_i (b_{i,t} + b_{i,t-u_i+1}) \le \sigma_t^{\mathrm{p}} \tag{26}$$

$$\sum_{i=1}^{m} \theta_i (b_{i,t} + b_{i,t-u_i+1}) \le \theta_t^{\mathrm{p}} \tag{27}$$

$$\sum_{i=1}^{m} \sum_{t \in Y} I_{i,t} \le \xi \tag{28}$$

where (13) shows the WT output power limit; (14) reflects the maintenance necessity limit; (15)-(17) are maintenance continuity limits; (18) implies the duration limit; (19) signifies the period limit; (20) means the deadline limit; (21) expresses the weather limit; (22) is the manpower limit; (23) and (24) signify vehicle limits; (25) indicates the greenhouse gas emission limit; (26) represents the marine environmental limit; (27) refers to the bird population limit; and (28) denotes the night maintenance limit.

4. Solution approach

The proposed model is a complex multi-objective nonlinear optimization problem. The nonlinear functions need to be reasonably linearized to reduce the difficulty of obtaining a solution and the multi-objectives can be processed by the ε-constraint method [30].

4.1. Linearization of wake model

The relationship between WT output power and wind speed is shown in Fig. 3. It can be expressed as

$$P_{i,t,\omega} = \begin{cases} 0 & ,0 \le v_{i,t,\omega} < v_i^{\mathrm{in}} \\ IF_i \cdot v_{i,t,\omega} + P_i^{\mathrm{z}} & ,v_i^{\mathrm{in}} \le v_{i,t,\omega} \le v_i^{\mathrm{r}} \\ P_i^{\mathrm{r}} & ,v_i^{\mathrm{r}} < v_{i,t,\omega} \le v_i^{\mathrm{out}} \\ 0 & ,v_{i,t,\omega} > v_i^{\mathrm{out}} \end{cases} \tag{29}$$

where IF_i, P_i^{z} are the slope and constant terms, respectively.

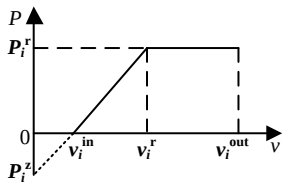

Fig. 3. Relationship between WT output power and wind speed

As shown in (1), the input wind speed of the WT is related to the maintenance state of upper WT and wake effect, which is a complicated mixed-integer nonlinear function. To simplify the calculation, for scenario ω, (1) can be equivalently transferred to:

$$v_{j,t,\omega}^2 = v0_{j,t,\omega}^2 - \sum_{i=1}^{n}(1-I_{i,t})\eta_{j,i,t,\omega}v0_{j,t,\omega}^2 + \sum_{i=1}^{n}\eta_{j,i,t,\omega}((1-I_{i,t})v_{j,i,t,\omega})^2 \tag{30}$$

where $\eta_{j,i,t,\omega}$, which is dependent on the wind direction and relative location of WTs, can be calculated by (7). The nonlinear part of (30) is then

$$\left((1-I_{i,t})v_{j,i,t,\omega}\right)^2 \tag{31}$$

By linearizing (31), it can be seen that

$$v1_{j,i,t,\omega} = (1-I_{i,t})v_{j,i,t,\omega} \tag{32}$$

$$s.t. \quad 0 \le v1_{j,i,t,\omega} \le v_{j,i,t,\omega} \tag{33}$$

$$(1-I_{i,t})M + v_{j,i,t,\omega} - M \le v1_{j,i,t,\omega} \le (1-I_{i,t})M \tag{34}$$

For the linearization of $v1_{j,i,t,\omega}^2$, this paper introduces auxiliary variable.

$$v2_{j,i,t,\omega} = v1_{j,i,t,\omega}^2 \tag{35}$$

Since the equality constraints are difficult to solve, (35) is relaxed into a second-order cone and formed the inequality, and this problem is transformed into a MISOCP problem.

$$(1-\rho)\frac{v2_{j,i,t,\omega}+1}{2} \le \sqrt{v1_{j,i,t,\omega}^2 + (\frac{v2_{j,i,t,\omega}-1}{2})^2} \le \frac{v2_{j,i,t,\omega}+1}{2} \tag{36}$$

where the value of ρ is small and taken as 10^{-2}.

To further speed up the solution, the second-order cone is approximately described as a polyhedron by the relaxation method [33], which transforms the MISOCP problem into a MILP problem. Taking the right part of (36) as an example, the processing can be described as:

$$\sqrt{v1_{j,i,t,\omega}^2+(\frac{v2_{j,i,t,\omega}-1}{2})^2}\le(1+\zeta)\frac{v2_{j,i,t,\omega}+1}{2} \tag{37}$$

$$v1_{j,i,t,\omega}\le\varphi_{j,i,t,\omega}^0 \tag{38}$$

$$\left|\frac{v2_{j,i,t,\omega}-1}{2}\right|\le\beta_{j,i,t,\omega}^0 \tag{39}$$

$$\varphi_{j,i,t,\omega}^k=\cos\frac{\pi}{2^{k+1}}\varphi_{j,i,t,\omega}^{k-1}+\sin\frac{\pi}{2^{k+1}}\beta_{j,i,t,\omega}^{k-1} \tag{40}$$

$$\beta_{j,i,t,\omega}^k\ge\left|-\sin\frac{\pi}{2^{k+1}}\varphi_{j,i,t,\omega}^{k-1}+\cos\frac{\pi}{2^{k+1}}\beta_{j,i,t,\omega}^{k-1}\right| \tag{41}$$

$$\varphi_{j,i,t,\omega}^K\le\frac{v2_{j,i,t,\omega}+1}{2} \tag{42}$$

$$\beta_{j,i,t,\omega}^K\le\tan\frac{\pi}{2^{k+1}}\varphi_{j,i,t,\omega}^K \tag{43}$$

where k=1,2,...,K; $\varphi_{j,i,t,\omega}^0$ and $\beta_{j,i,t,\omega}^0$ are auxiliary variables.

(38)-(43) show the polyhedral approximation obtained by the relaxation method. Due to the equality constraint of $\varphi_{j,i,t,\omega}^0$, $\beta_{j,i,t,\omega}^{k-1}$, and $\varphi_{j,i,t,\omega}^k$ are given by (40) , K equality constraints and K variables $\varphi_{j,i,t,\omega}^k$ can be eliminated by substituting (40) into the rest equations. The second-order cone constraint for variables $v1_{j,i,t,\omega}$ and $v2_{j,i,t,\omega}$ in the optimization problem is approximately equivalent to the linear inequality constraints constructed by a set of variables $v1_{j,i,t,\omega}$, $v2_{j,i,t,\omega}$, $\varphi_{j,i,t,\omega}^0$, and (K+1) variables $\beta_{j,i,t,\omega}^k$. Therefore, the second-order cone programming problem is transformed into a linear programming problem. Further, the slack variable ζ can be expressed as:

$$\zeta=\frac{1}{\cos(\frac{\pi}{2^{K+1}})^2}-1 \tag{44}$$

The smaller the value of ζ , the higher the accuracy of the second-order cone approximate description. In this paper, K=11 is chosen for solving and ζ=6×10^{-7} is obtained. Thus, the value of ζ is small enough to make the main aspects of (36) are kept. The processing is similar for the left part of (36).

In addition, the auxiliary variable $v3_{j,t,\omega}$ is introduced to calculate $v_{j,t,\omega}^2$ in (30),

$$v3_{j,t,\omega} = v0_{j,t,\omega}^2 - \sum_{i=1}^{n}(1-I_{i,t})\eta_{j,i,t,\omega}v0_{j,t,\omega}^2 + \sum_{i=1}^{n}\eta_{j,i,t,\omega}v2_{j,i,t,\omega} \tag{45}$$

It can be found that

$$v3_{j,t,\omega} = v_{j,t,\omega}^2 \tag{46}$$

The linearization of (46) is the same as described for (35). Moreover, the thrust coefficient $C_{i,t}^{\mathrm{T}}$ in (2) can be approximately expressed [15] as:

$$C_{i,t,\omega}^{\mathrm{T}} = k^{\mathrm{z}}v_{i,t,\omega} + b^{\mathrm{z}} \tag{47}$$

where both k^{z} and b^{z} can be obtained by fitting the curve of thrust coefficient vs. wind speed.

Because $k_{j,i}$ is determined by WTs spacing and the impeller diameter of WT i, it can be formulated in advance and is independent of the optimization variables. The only nonlinear part of (2) is $v_{i,t,\omega}^2$, which was linearized in the preceding calculations. Then, the linearization of the wake model can be accomplished by the above methods.

4.2. Processing of multi-objective function

To solve the proposed model, the ε-constraint method [30] is used to deal with the multi-objective function. The f_1 optimization direction is minimized and the f_2 optimization direction is maximized as follows:

Step 1: Input the original data of the model and solve each single objective optimization model. This will generate the objective function values and optimization decision variables for different optimization targets, respectively. Then the range of ε_γ (γ=1, 2) can be determined by the function values obtained.

Step 2: Substitute ε_γ into the corresponding objective function to generate a constraint. Based on this, the multi-objective function is transformed into a single objective function and MILP method is applied to solve.

Step 3: Repeat Step 2 by selecting different values of ε_γ and the Pareto optimal solutions of the model can be obtained.

To sum up, the flowchart of solving the optimization model of maintenance scheduling for offshore wind turbines considering the wake effect is shown as Fig. 4.

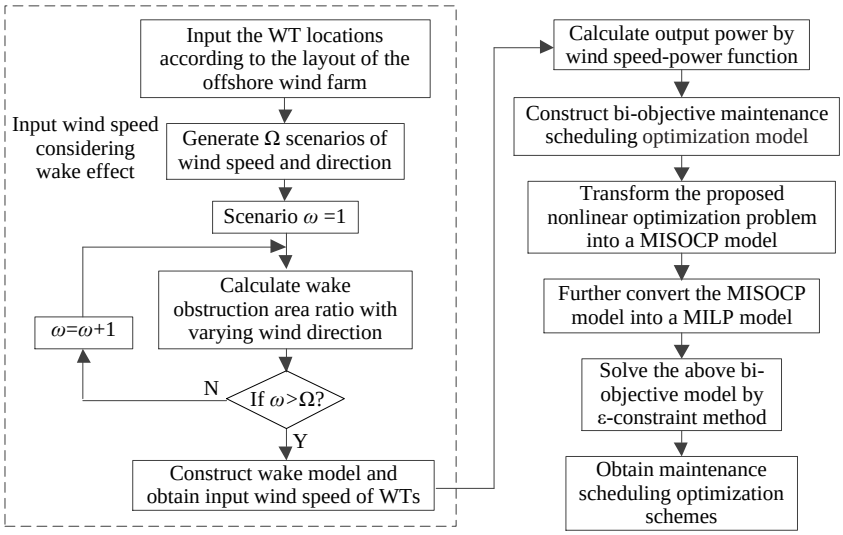

Fig. 4. The flowchart of solving the optimization model of maintenance scheduling

5. Case Studies

The specific layout of the offshore wind farm considered in this paper is shown in Fig. 5. There are 30 WTs that are numbered 1 to 30. The rated power of each WT is 3 MW, the impeller radius is 63 m, and the row and column spacings are both 560 m. The WT cut-in speed is 3 m/s, the rated wind speed is 13 m/s, and the cut-out wind speed is 25 m/s. The time horizon for optimization scheduling is one week, with 1 hour for a time period and totally 168 time periods. The expected values of wind speed and wind direction for each time period are shown in Fig. 6 and the prediction error does not exceed 10%. A total of 10 WTs need to be maintained (numbered 1, 2, 3, 4, 5, 6, 8, 11, 12, and 15) in the offshore wind farm and the maintenance period starts at 6 a.m. The maintenance duration of the 1st and 11th WTs is 10 time periods, while other WTs require 8 time periods. The relevant parameters in the model such as cost, manpower demand, etc. can be found in [5] and [24]. The maintenance deadline of the 3rd WT is the 50th period. The 5th and 15th WT cannot be maintained at the same time.

As the number of scenarios increases, model calculation becomes more complicated. This paper reduces the 2000 scenarios generated by LHS to 20 for case studies to investigate the effectiveness of the proposed model and method. The tests are carried out on a laptop with an Intel Core i5 2.50 GHz CPU and 8 GB of RAM using a MATLAB and GAMS platform. Related cases are illustrated as follows.

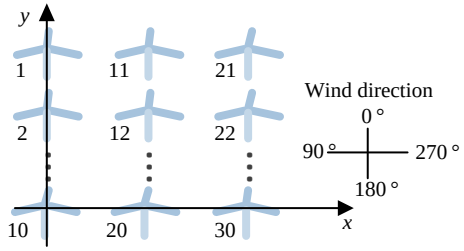

Fig. 5. The layout of the offshore wind farm

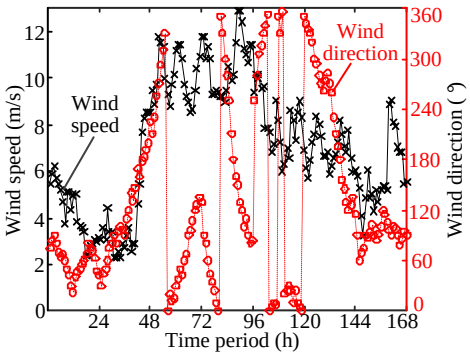

Fig. 6. Expected values of wind speed and wind direction

5.1. Influence of wind direction on wake effect

To show the impact of wind direction change on the wake effect, the 4th day with relatively extensive wind direction coverage is selected and the following four cases are considered for comparison as well as wind speed dates employ the expected values of the 4th day.

Case 1: Wind direction is 0 °;

Case 2: Wind direction is 90 °;

Case 3: Wind direction is 30 °;

Case 4: Consistent with the expectations of the wind direction on the 4th day.

Fig. 7 shows the output power of the WTs in each period, and Fig. 8 compares the output power of each WT for the different cases. The output power of case 4 varies greatly in Fig. 7, which indicates that the change of wind direction has a great influence on the output power of the wind farm. In addition, the wind farm output power is lower when the wind direction is near 0 ° and higher when near 90 °. The reason, which can be found from Fig. 8, is that the wake effect is more pronounced at 0 °, which makes the wind farm output power drop further. In case 3, the output power is also large. However, the difference in the WT output at 30 ° is significant in Fig. 8. Although some WTs are not affected by the

wake, the 25th-30th WTs have low outputs that are influenced by the wake superposition of multiple WTs, which limits the overall output power of the offshore wind farm.

Moreover, comparing the curves in Fig. 8 shows the output power of each WT in case 4 is more uniform and more in line with the actual operating conditions of offshore WTs. The above indicates the rationality and feasibility of the proposed wake model in this paper, which can adapt to the actual wind speed and wind direction change. The output power of the offshore wind farm can be described more objectively in the case study by adopting varying wind direction.

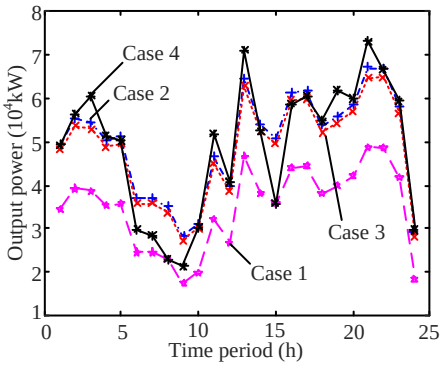

Fig. 7. Wind farm output power for various time periods

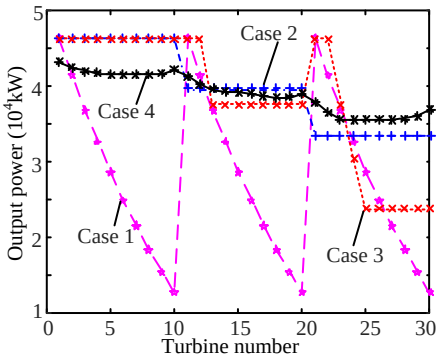

Fig. 8. Output power of each WT

5.2. Optimization of maintenance scheduling

1) Maintenance scheduling

For maintenance scheduling, it is necessary to optimize both maintenance costs and power generation to achieve the greatest economic benefits. According to the part 3 in Section 4, the Pareto optimal solutions of this problem can be obtained.

Table 2 shows the values of Pareto optimal solutions obtained by MILP method. It can be seen that when the maintenance cost reduces, the power generation also decreases. It means that the trend of maintenance cost decreasing and power generation increasing is inconsistent in the optimization.

Therefore, it is necessary to consider the two objectives of minimizing maintenance costs and maximizing power generation to make the decision of the maintenance scheduling. Taking one of the Pareto optimal solutions for example, such as the 11th solution, the optimized maintenance cost of offshore WTs is \$374,600 and the generation is 5.375×10^6 kWh; the corresponding maintenance scheduling is shown in Fig. 9. The magnified windows are to show the hour No. of maintenance scheduling in detail.

Table 2

Values of Pareto optimal solutions

No.	f_1 (10^4 \$)	f_2 (10^6 kWh)	No.	f_1 (10^4 \$)	f_2 (10^6 kWh)
1	37.040	5.276	11	37.460	5.375
2	37.056	5.285	12	37.582	5.381
3	37.083	5.291	13	37.665	5.392
4	37.112	5.304	14	37.736	5.399
5	37.152	5.309	15	37.793	5.410
6	37.236	5.328	16	37.912	5.417
7	37.254	5.332	17	37.965	5.421
8	37.325	5.345	18	38.050	5.428
9	37.388	5.357	19	38.124	5.435
10	37.433	5.366	20	38.231	5.438

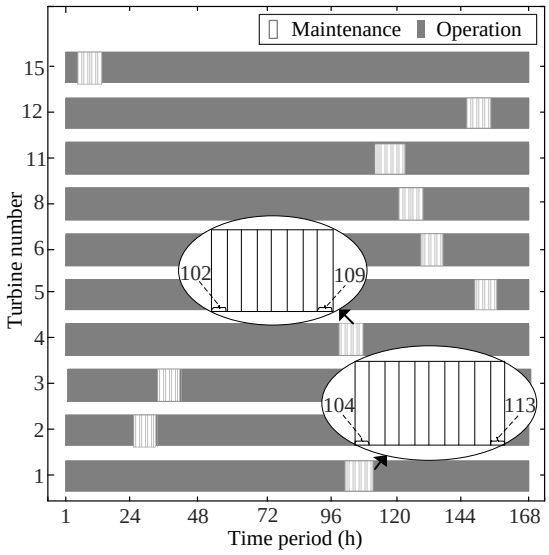

Fig. 9. The maintenance arrangement of WTs

Fig. 9 illustrates that the maintenance periods of WTs are mostly distributed in the 25th-38th, 102nd-135th, and 146th-154th periods, most of which are during the daytime because of the relatively low maintenance cost. But, taking into account the continuity, some of the maintenance periods are still at night. Taken together, the maintenance period is not always scheduled to coincide with low wind speeds.

In some periods, the wind speed is obviously high, but the wind direction is around 0°, which results in the WT having a low output power. Maintenance during these periods will achieve better economic benefits. In addition, due to restrictions on manpower, maintenance vessels, and helicopters in each period, maintenance work on the WTs is not concentrated in several time periods; rather, it fits the actual situation of maintenance for offshore WTs.

2) The impact of maintenance status on wake distribution

When the WT is in maintenance, it does not absorb wind energy. Thus, the wake effect among the WTs will change and will affect the output power of downstream WTs. Taking the 4th WT as an example, with the maintenance scheduling shown in Fig. 9, its maintenance periods are 102nd-109th periods. And the output power of its downstream 5th WT is calculated in two scenarios: with or without consideration of the impact of the upstream WT maintenance on wake distribution, respectively. The result is shown in Fig. 10.

Fig. 10 demonstrates that when the WT is in maintenance, the impact of the wake on the downstream WT will be enhanced and the output power of the downstream WT will increase. By calculation and analysis, the total output of the 5th WT with and without consideration of maintenance state is 6680.04 and 5710.67 kW, respectively. The former represents about 17% more output power than the latter for the 5th WT only. Simultaneously, the wake effect of the 5th WT has an impact on the output power of other WTs. Therefore, the impact of the maintenance state cannot be ignored, and should be considered to more exactly describe the output power of the downstream WTs during maintenance periods.

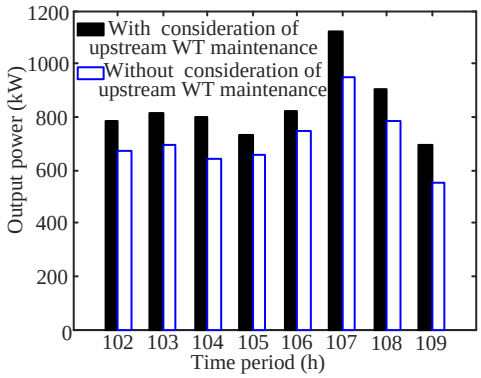

Fig. 10. Output power of the downstream 5th WT with different scenarios

5.3. Method validation

1) Comparison with NSGA-II algorithm

In order to verify the advantage of the proposed MILP method, it is compared with the widely used NSGA-II algorithm [24] and the results are shown in Fig. 11. It shows that the Pareto optimal solution sets obtained by the two methods are relatively close. However, the search space of the MILP method is wider and can obtain the range of the objective function f_1<37.2×10^4 \$, which further improves the quality of the optimal solution set. In addition, NSGA-II has a long calculation time, which is 736.58 s. In comparison, the MILP method takes 161.20s, which can save 78.1% of the calculation time.

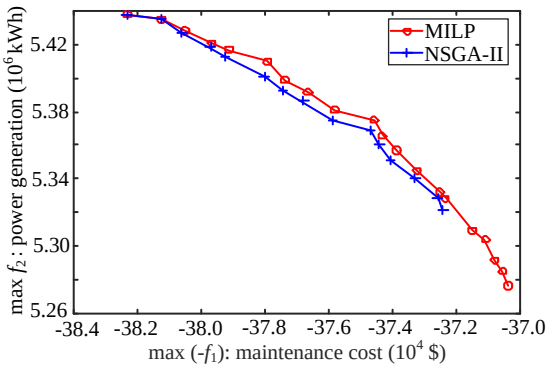

Fig. 11. Results comparison of MILP method and NSGA-II

2) Comparison with MISOCP method

To further verify the performance of the proposed MILP method, the optimization results of the maintenance scheduling obtained by MISOCP in [27] are utilized as reference and compared. The relative deviation of the obtained 20 groups of Pareto optimal solutions and the saved calculation time of MILP are shown in Fig. 12. For each Pareto optimal solution listed in Table 2, the relative deviations of maintenance costs and power generation are not more than 0.023% and 0.024%, respectively. The computing time of the two methods differs greatly. Compared with MISOCP method, calculation time of MILP method can save 66%-79% and the average calculation time of the MILP method is 8.06 s. Consequently, the solution accuracy is almost the same under the two methods, but the MILP method obviously has a great advantage in terms of solving efficiency.

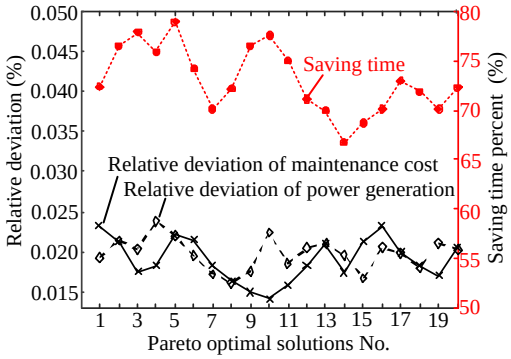

Fig. 12. Results comparison between MILP and MISOCP

5.4. Solutions for offshore wind farms of different scales

In order to verify the feasibility and adaptability of the proposed model, large-scale case studies are conducted. The scale of the original wind farm is doubled, tripled, and quadrupled for example analysis, respectively. The layouts of each wind farm are shown in Fig. 13 and WTs distributions are 10 rows and 3 columns, 10 rows and 6 columns, 10 rows and 9 columns, and 10 rows and 12 columns. The solution results are shown in Fig. 14 for these 4 offshore wind farms of different scales. Fig.14 indicates that with the expansion of the offshore wind farm scale, the power generation obviously increases, and the maintenance cost gradually decreases. When the number of WTs is large in a wind farm, the wake effect is more pronounced. In this case, more downstream WTs will be able to utilize the wind energy as the wake distribution changes while the upstream WT is in maintenance, which makes the overall shutdown loss of the wind farm smaller, and the maintenance cost reduces. Therefore, the maintenance scheduling optimization model proposed in this paper is still applicable to a large-scale offshore wind farm.

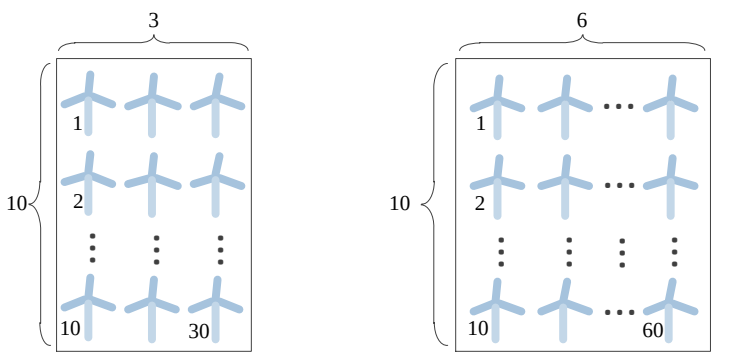

a) Wind farm with 30 WTs b) Wind farm with 60 WTs

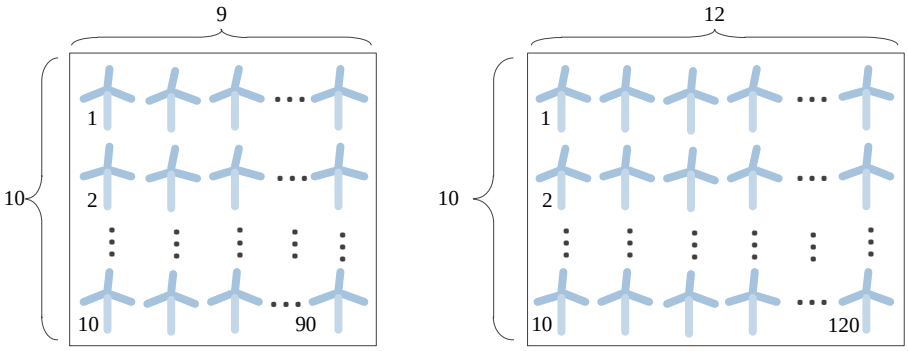

c) Wind farm with 90 WTs d) Wind farm with 120 WTs

Fig. 13. Layout of 4 offshore wind farms

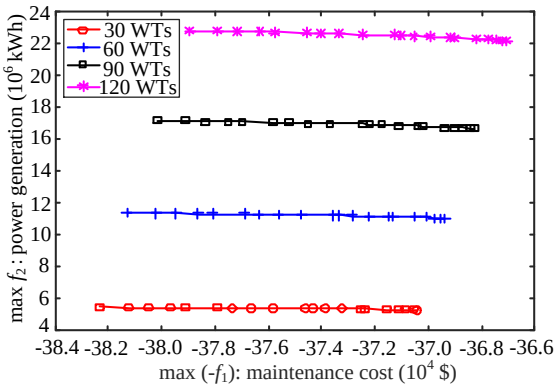

Fig. 14. Solution results for offshore wind farms of different scales

6. Conclusions

This paper proposes an optimization scheduling model for the maintenance of offshore wind farms. The model considers the wake effect of arbitrary wind direction, influence of maintenance status on output power, and economic performance with maximum power generation and minimum maintenance costs. The proposed process incorporates MISOCP and MILP methods as well as the ε-constraint method. Through theoretical analysis and case studies, this paper shows that:

a) Both the wind direction and maintenance status of a WT have a significant influence on the wake effect, which affects the output power of the offshore wind farm. Through the wake model proposed, the output power can be accurately reflected in the time horizon considered.

b) Maintenance scheduling with optimal comprehensive economic benefits considering the uncertainty of wind speed and direction can be obtained by utilizing MILP and the ε-constraint method to solve the proposed model, which provides a reference for the schematization of maintenance of the offshore WTs.

c) The proposed second-order cone of the wake model is approximately described as a polyhedron, which allows the MISOCP problem to be represented as multiple linear inequalities. The algebraic modelling method is utilized to linearize the remaining nonlinear coupling relationships to form a new model solved by MILP method. The simulation results show that compared with NSGA-II and MISOCP methods, the proposed method can improve the solution efficiency while ensuring the high quality of the solution.

7. Acknowledgements

This work was supported in part by a National Natural Science Foundation of China grant (No. 51507100), a Shanghai Engineering Research Center of Green Energy Grid-Connected Technology grant (No. 13DZ2251900), and the “Electrical Engineering” Shanghai class II Plateau Discipline.

8. References

[1] L. Huang, Y. Fu, Y. Mi, J. Cao, and P. Wang, A Markov-Chain-based availability model of offshore wind turbine considering accessibility problems, IEEE Trans. Sust. Energy 8 (4) (2017) 1592-1600. https://doi.org/10.1109/TSTE.2017.2695661.

[2] M. Hofmann and I. B. Sperstad, NOWIcob – A tool for reducing the maintenance costs of offshore wind farms, Energy Procedia 35 (2013) 177-186. https://doi.org/10.1016/j.egypro.2013.07.171.

[3] I. Fonseca, J. T. Farinha, and F. M. Barbosa, Maintenance planning in wind farms with allocation of teams using genetic algorithms, IEEE Lat. Am. Trans. 12 (6) (2014) 1062-1070. https://doi.org/10.1109/TLA.2014.6894001.

[4] J. Nilsson and L. Bertling, Maintenance management of wind power systems using condition monitoring systems—life cycle cost analysis for two case studies, IEEE Trans. Energy Conver. 22 (1) (2007) 223-229. https://doi.org/10.1109/PES.2007.385616.

[5] Y. Dalgic, I. Lazakis, I. Dinwoodie, D. McMillan, and M. Revie, Advanced logistics planning for offshore wind farm operation and maintenance activities, Ocean Eng. 101 (2015) 211-226. https://doi.org/10.1016/j.oceaneng.2015.04.040.

[6] A. H. Schrotenboer, A. J. Michiel, B. Jargalsaikhan, and K. J. Roodbergen, Coordinating technician allocation and maintenance routing for offshore wind farms, Comput. Oper. Res. 98 (2018) 185-197. https://doi.org/10.1016/j.cor.2018.05.019.

[7] P. F. Odgaard, J. Stoustrup and M. Kinnaert, Fault-tolerant control of wind turbines: a benchmark model, IEEE Trans. Contr. Syst. T. 21 (4) (2013) 1168-1182. https://doi.org/10.1109/TCST.2013.2259235.

[8] P. F. Odgaard and J. Stoustrup, Fault tolerant wind farm control — A benchmark model, 2013 IEEE International Conference on Control Applications (CCA), Hyderabad, (Aug) (2013) 412-417. https://doi.org/10.1109/CCA.2013.6662784.

[9] E. Sales-Setién and I. Peñarrocha-Alós, Multiobjective performance-based designs in fault estimation and isolation for discrete-time systems and its application to wind turbines, Int. J. Syst. Sci. 50 (6) (2019) 1252-1274. https://doi.org/10.1080/00207721.2019.1598511.

[10] E. Sales-Setién and I. Peñarrocha-Alós, Markovian jump system approach for the estimation and adaptive diagnosis of decreased power generation in wind farms, IET Control Theory A. 13 (18) (2019) 3006-3018. https://doi.org/10.1049/iet-cta.2018.6199.

[11] E. Sales-Setién and I. Peñarrocha-Alós, Robust estimation and diagnosis of wind turbine pitch misalignments at a wind farm level, Renewable Energy 146 (2020) 1746-1765. https://doi.org/10.1016/j.renene.2019.07.133.

[12] G. Ji, W. Wu, and B. Zhang, Robust generation maintenance scheduling considering wind power and forced outages, IET Renew. Power Gen. 10 (5) (2016) 634-641. https://doi.org/10.1049/iet-rpg.2015.0198.

[13] E. Byon, E. Perez, and Y. Ding, Simulation of wind farm operations and maintenance using discrete event system specification, SIMUL.-Trans. Soc. Mod. Sim. 87 (12) (2011) 1093-1117. https://doi.org/10.1177/0037549711376841.

[14] P. G. Mikel, G. B. Oriol, S. Andreas, and B. J. Joan, Analysis of a multi turbine offshore wind farm connected to a single large power converter operated with variable frequency, Energy 36 (5) (2011) 3272-3281. https://doi.org/10.1016/j.energy.2011.03.020.
[15] H. Kim, C. Singh, and A. Sprintson, Simulation and estimation of reliability in a wind farm considering the wake effect, IEEE Trans. Sust. Energy 3 (2) (2012) 274-282. https://doi.org/10.1109/tste.2011.2174260.
[16] C. Hwang, J. H. Jeon, and G. H. Kim, Modelling and simulation of the wake effect in a wind farm, J. Int. Council Electr. Eng. 5 (1) (2015) 74-77. https://doi.org/10.1080/22348972.2015.1109793.
[17] F. González-Longatt, P. Wall, and V. Terzija, Wake effect in wind farm performance: Steady-state and dynamic behavior, Renewable Energy 39 (1) (2012) 329-338. https://doi.org/10.1016/j.renene.2011.08.053.
[18] A. Feijoo and D. Villanueva, Contributions to wind farm power estimation considering wind direction-dependent wake effects: Wind farm power estimation, Wind Energy 20 (2) (2017) 221-231. https://doi.org/10.1002/we.2002.
[19] H. Yang, K. Xie, H. Tai, and Y. Chai, Wind farm layout optimization and its application to power system reliability analysis, IEEE Trans. Power Syst. vol. 31, 31 (3) (2016) 2135-2143. https://doi.org/10.1109/TPWRS.2015.2452920.
[20] M. Abbes and M. Allagui, Centralized control strategy for energy maximization of large array wind turbines, Sustain. Cities Soc. 25 (2016) 82-89. https://doi.org/10.1016/j.scs.2015.11.007.
[21] Y. Wu, C. Lee, C. Chen, K. Hsu, and H. Tseng, Optimization of the wind turbine layout and transmission system planning for a large-scale offshore wind farm by AI technology, IEEE Trans. Ind. Appl. 50 (3) (2014) 2071-2080. https://doi.org/10.1109/IAS.2012.6373997.
[22] J. Shin and J. Kim, Optimal design for offshore wind farm considering inner grid layout and offshore substation location, IEEE Trans. Power Syst. 32 (3) (2017) 2041-2048. https://doi.org/10.1109/TPWRS.2016.2593501.
[23] P. Hou, W. Hu, M. Soltani, and Z. Chen, Optimized placement of wind turbines in large-scale offshore wind farm using particle swarm optimization algorithm, IEEE Trans. Sust. Energy 6 (4) (2015) 1272-1282. https://doi.org/10.1109/TSTE.2015.2429912.
[24] S. Y. Zhong, A. Pantelous, M. Beer, and J. Zhou, Constrained non-linear multi-objective optimisation of preventive maintenance scheduling for offshore wind farms, Mech. Syst. Signal Pr. 104 (2018) 347-369. https://doi.org/10.1016/j.ymssp.2017.10.035.
[25] Z. Dar, K. Kar, O. Sahni, and J. H. Chow, Wind farm power optimization using yaw angle control, IEEE Trans. Sust. Energy 8 (1) (2017) 104-116. https://doi.org/10.1109/TSTE.2016.2585883.
[26] A. Nikoobakht, J. Aghaei, T. Niknam, V. Vahidinasab, H. Farahmand, and M. Korpås, Towards robust OPF solution strategy for the future AC/DC grids: case of VSC-HVDC-connected offshore wind farms, IET Renew. Power Gen. 12 (6) (2018) 691-701. https://doi.org/10.1049/iet-rpg.2017.0575.
[27] T. Ding, S. Liu, W. Yuan, Z. Bie, and B. Zeng, A two-stage robust reactive power optimization considering uncertain wind power integration in active distribution networks, IEEE Trans. Sust. Energy 7 (1) (2016) 301-311. https://doi.org/10.1109/TSTE.2015.2494587.
[28] Y. Chen, Z. Y. Dong, K. Meng, F. Luo, Z. Xu, and K. P. Wong, Collector system layout optimization framework for large-scale offshore wind farms, IEEE Trans. Sust. Energy 7 (4) (2016) 1398-1407. https://doi.org/10.1109/TSTE.2016.2549602.
[29] J. D. Álvaro, D. C. Edgardo, S. Ismael, and U. Julio, Optimal operation of a pumped-storage hydro plant that compensates the imbalances of a wind power producer, Electr Pow. Syst. Res. 81 (9) (2011) 1767-1777. https://doi.org/10.1016/j.epsr.2011.04.008.
[30] G. Mavrotas, Effective implementation of the ε-constraint method in multi-objective mathematical programming problems, Appl. Math. Comput. 213 (2) (2009) 455-465. https://doi.org/10.1016/j.amc.2009.03.037.
[31] R. S. Ferreira, C. L. T. Borges, and M. V. F. Pereira, A flexible mixed-integer linear programming approach to the AC optimal power flow in distribution systems, IEEE Trans. Power Syst. 29 (5) (2014) 2447-2459. https://doi.org/10.1109/tpwrs.2014.2304539.
[32] J. Xu, X. Yi, Y. Sun, T. Lan, and H. Sun, Stochastic optimal scheduling based on scenario analysis for wind farms, IEEE Trans. Sust. Energy 8 (4) (2017) 1548-1559. https://doi.org/10.1109/tste.2017.2694882.
[33] B. T. Aharon and N. Arkadi, On polyhedral approximations of the second-order cone, Math. Oper. Res. 26 (2) (2001) 193-205. https://doi.org/10.1287/moor.26.2.193.10561.
[34] Y. Wu, P. Su, Y. Su, T. Wu, and W. Tan, Economics- and reliability-based design for an offshore wind Farm, IEEE Trans. Ind. Appl. 53 (6) (2017) 5139-5149. https://doi.org/10.1109/TIA.2017.2737399.
[35] M. Yildirim, N. Z. Gebraeel and X. A. Sun, Integrated predictive analytics and optimization for opportunistic maintenance and operations in wind farms, IEEE Trans. Power Syst. 32 (6) (2017) 4319-4328. https://doi.org/10.1109/TPWRS.2017.2666722.
[36] A. Chandra, O. Djamila, J. Dylan, S. Magnus and B. S. Iver, Optimisation of maintenance routing and scheduling for offshore wind farms, Eur. J. Oper. Res. 256 (1) (2017) 76-89. https://doi.org/10.1016/j.ejor.2016.05.059.
[37] Z. Y. Zhang, Scheduling and routing optimization of maintenance fleet for offshore wind farms using Duo-ACO, Adv. Mater. Res. 1039 (2014) 294-301. https://doi.org/10.4028/www.scientific.net/AMR.1039.294.
[38] C. A. Irawan, M. Eskandarpour, D. Ouelhadj, and D. Jones, Simulation-based optimisation for stochastic maintenance routing in an offshore wind farm, Eur. J. Oper. Res. (2019).

https://doi.org/10.1016/j.ejor.2019.08.032.
[39] D. M. Fan, Y. Ren, Q. Feng, B. Y. Zhu, Y. Liu, and Z. L. Wang, A hybrid heuristic optimization of maintenance routing and scheduling for offshore wind farms, J. Loss Prevent. Proc. 62 (2019). https://doi.org/10.1016/j.jlp.2019.103949.
[40] F. Besnard, K. Fischer, and L. B. Tjernberg, A model for the optimization of the maintenance support organization for offshore wind farms, IEEE Trans. Sust. Energy 4 (2) (2013) 443-450. https://doi.org/10.1109/TSTE.2012.2225454.
[41] M. Gaumond, P. E. Réthoré, S. Ott, and P. S. Andrea, Evaluation of the wind direction uncertainty and its impact on wake modeling at the Horns Rev offshore wind farm, Wind Energy 17 (8) (2014) 1169-1178. https://doi.org/10.1002/we.1625.
[42] D. Madjidian and A. Rantzer, A stationary turbine interaction model for control of wind farms, IFAC Proceedings Volumes 44 (1) (2011) 4921-4926. https://doi.org/10.3182/20110828-6-it-1002.00267.
[43] H. Aksoy, Z. Toprak, A. Aytek, and N. Ünal, Stochastic generation of hourly mean wind speed data, Renewable Energy 29 (14) (2004) 2111-2131. https://doi.org/10.1016/j.renene.2004.03.011.
[44] Z. Shu, P. Jirutitijaroen, A. M. Leite da Silva, and C. Singh, Accelerated state evaluation and latin hypercube sequential sampling for composite system reliability assessment, IEEE Trans. Power Syst. 29 (4) (2014) 1692-1700. https://doi.org/10.1109/TPWRS.2013.2295113.
[45] L. Wu, M. Shahidehpour and T. Li, Stochastic Security-Constrained Unit Commitment, IEEE Trans. Power Syst. 22 (2) (2007) 800-811. https://doi: 10.1109/TPWRS.2007.894843.

Xiaolin Ge received the M.S. degree and Ph.D. in Electrical Engineering from North China Electric Power University, Beijing, China, in 2010 and 2013, respectively. In 2013, she joined the Shanghai University of Electric Power, where she is an associate professor. Her research interests include offshore wind power, optimization of large-scale systems and scheduling of cascaded hydro power systems.(Email: gexiaolin2005@126.com)

Quan Chen is studying for a Master's degree in Electrical Engineering from Shanghai University of Electric Power, Shanghai, China. His research interests are operation and maintenance strategy of offshore wind turbines.(Email: chenquan95@163.com)

Yang Fu received the Ph.D. degree from Shanghai University, Shanghai, China, in 2005. Currently he is a Professor and the head of Electrical Engineering College at Shanghai University of Electric Power. His special fields of interest include power system planning, operation and control, and renewable energy.(Email: mfudong@126.com)

C. Y. Chung received the B.Eng. (with First Class Honors) and Ph.D. degrees in electrical engineering from The Hong Kong Polytechnic University, Hong Kong, China, in 1995 and 1999, respectively. He has worked for Powertech Labs, Inc., Surrey, BC, Canada; the University of Alberta, Edmonton, AB, Canada; and The Hong Kong Polytechnic University, China. He is currently a Professor, the NSERC/SaskPower (Senior) Industrial Research Chair in Smart Grid Technologies, and the SaskPower Chair in Power Systems Engineering in the Department of Electrical and Computer Engineering at the University of Saskatchewan, Saskatoon, SK, Canada. His research interests include smart grid technologies, renewable energy, power system stability/control, planning and operation, computational intelligence applications, and power markets. Dr. Chung is an Editor of IEEE Transactions on Power Systems, IEEE Transactions on Sustainable Energy, and IEEE Power Engineering Letters. He is also a member of the IEEE PES Fellow Evaluation Committee.(Email: c.y.chung@usask.ca)

Yang Mi received the Ph.D. degree from Northeastern University, Shenyang, China, in 2005. Currently she is a Professor with Shanghai University of Electric Power, Shanghai. Her research interests include power system control and protection.(Email: miyangmi@163.com)